

# Experimental Characterization of MCF-10A Normal Cells Using AFM: Comparison with MCF-7 Cancer Cells

Moharam Habibnejad Korayem<sup>1,\*</sup> and Zahra Rastegar<sup>2</sup>

<sup>1</sup>Mechanical Engineering, School of Mechanical Engineering, Iran University of Science and Technology, Narmak, Tehran.

<sup>2</sup>Candidate of Mechanical Engineering, School of Mechanical Engineering, Iran University of Science and Technology, Narmak, Tehran.

\*Corresponding Author: Moharram Habibnejad Korayem. Email: Hkorayem@iust.ac.ir.

**Abstract:** The mechanical properties of single cells have been recently identified as the basis of an emerging approach in medical applications since they are closely related to the biological processes of cells and human health conditions. The problem in hand is how to measure mechanical properties in order to obtain them more accurately and applicably. Some of the cell's properties such as elasticity module and adhesion have been measured before using various methods; nevertheless, comprehensive tests for two healthy and cancerous cells have not been performed simultaneously. As a Nanoscale device, AFM has been used for some biological cells, however for breast cells, it has been utilized just to measure elasticity module. To provide a more accurate comparison for the healthy and the malignant cancer cells of breast, mechanical properties of MCF-10A cells such as topography, elasticity module, adhesion force, viscoelastic characteristics, bending and axial rigidity were determined and compared to the MCF-7 cells results obtained in previous works. Results revealed that the healthy breast cells are stiffer and less adhesive in comparison with the cancerous ones. Topography images revealed that cancerous cells have bigger radii. These results can help with the diagnosis of malignant cancer cells and even the level of the disease.

**Keywords:** Healthy breast cell; breast malignant cancer cell; cell mechanical properties; atomic force microscopy

## 1 Introduction

Through the increasingly growing breast cancer occurrence and the importance of its prevention and diagnosis, many different methods have been used to tackle it. There are various devices hired to measure biological cell's different properties, one of which is atomic force microscopy (AFM) [16]. The advantage of AFM over other methods is its capability to present information about other properties such as adhesion distribution, friction, elasticity module, viscoelastic characteristics and surface topography [10]. AFM function in the case of soft surfaces, such as cells and polymers, has some complexities; Weisenhorn et al. obtained force-distance and force-indentation depth curves for elastomers, rubbers and biological cells in contact moments and extracted the parabolic curves. Then the elasticity module was obtained according to the existing theory. Finally, the force range in which the best clarity existed was represented [20].

Vinckier and Semenza measured the elasticity module of biological materials using AFM. Utilizing Hertz theory, they extracted the way to obtain elasticity module and then attempted to measure it for biological cells and soft matters via AFM [19]. Ikai et al. reviewed Nano-mechanical methods using AFM; they obtained the elasticity module using Hertz theory and indentation data [7]. Park and Lee measured mechanical properties in three distinctive parts of a Muller cell. To do so, the AFM tip was put in touch with three separate parts of the cell so that the force-indentation depth curves were extracted [14].

Adhesion force behavior can be related to van der Waals and capillary forces between AFM tip and surface. There is no capillary force in dry or vacuum environments; otherwise, due to the environment

humidity, there will be a capillary force, which affects the interaction between tip and surface. The capillary force magnitude depends on the tip-sample distance. The magnitude and direction of the force inserted by the cantilever are related to its deviation and spring constant value [13].

The most basic applications of AFM are geometry, mechanical properties recognition and manipulation of biological cells. Kasas et al. studied mechanical properties such as elasticity module, poisson's ratio and adhesion of biological cells such as virus, bacteria, yeast, herbal cells and some mammalian cells by AFM [8]. Li et al. calculated that the mechanical properties of the red blood cell and three distinct types of cancer cells using AFM. Force-displacement curves showed that the elasticity module of a red blood cell, as well as its diameter, is less than those of three types of cancer cells [11].

Lee et al. calculated the breast cancer cells properties using force-displacement curves obtained by AFM. Results illustrated that the elasticity module for breast cancer cells is lower than the one of a healthy cell [12]. Faria et al. tried imaging and recognition of three different types of prostate cancer cells' properties. Cancer cells were cultivated in different days and Hertz spherical elastic theory was used for force-displacement experimental curve [3]. Hui et al. represented a contact model for viscoelastic spheres using the JKR model. Their numerical simulation was confirmed by the previous experimental results [6].

Cartagena and Raman investigated the local viscoelastic properties of living cells using dynamic and quasi-static models based on AFM. In this study, the force gradient and losses on fibroblast cells in buffer solutions were reconstructed using Lorentz force-excited cantilevers. Finally, stiffness and viscoelastic properties were measured locally and the difference between the spring force and the viscosity of material were obtained [1]. Zhai and McKenna modeled the viscoelastic contact problem of Nano-sphere and polyester surface in indentation tests. Illustrating limitations of the analysis achieved just by one load indentation curve, they represented that this method does not suffice for determining total range of polymer viscoelastic response [21].

According to different internal parts of cell and various arrangements of them based on cell properties and their floatation inside the cell cytoplasm, it is possible that cell mechanical properties in different points would be different; on this path Park and Lee investigated Muller cell's local changes of elasticity modulus using AFM [14].

Biochemical therapies effect on cell-cell adhesion and individual cell mechanics was investigated by AFM. The tip-less cantilever was used to connect cells. Cell-cell adhesion parameters such as maximum separation force and work of adhesion were extracted from the force-displacement curves. Puech et al. measured adhesion properties of zebrafish single cells to substrates and concluded that extracellular connections affect intracellular signaling [15].

In this paper, mechanical properties of healthy and cancerous breast cells were extracted using existing theories and experimental data from AFM tests. Then they were processed using AFM software, Matlab and Microsoft Excel. The novelties of the work include a comprehensive comparison between MCF-7 and MCF-10A cells' mechanical properties using atomic force microscopy as a nanoscale device. Viscoelasticity parameters of cells have been extracted which can be applied in modeling of the contact moment and manipulation process. These properties include elasticity and viscosity of the cell and also its creep function which can be applied in mechanical models to provide more accurate modeling and simulation of the contact moment and the manipulation process. Moreover, adhesion of the cell to the AFM tip has been investigated; applicable in the estimation of the sliding moment of the tip on the cell during manipulation. In general, results are important for the diagnosis of cancerous cells which can help avoid the disease' progress. Besides, since this research is the basis of the further researches such as cell manipulation to the specified point and using results for in vitro and in vivo procedures, other mechanical properties needed such as bending and axial rigidity were also extracted. All these tests have been performed on three different points to find the best point for starting the manipulation which avoids cells' damage.

## 2 Theory

In this section, theories have been used to estimate the mentioned parameters that are explained. In these theories, assumptions are applied to simplify the calculation process.

### 2.1 Biological Cell Elasticity Module

In order to calculate cell elasticity module, force-indentation depth equations of the contact model should be rewritten in terms of elasticity module. While tested cells have extended geometries, to simplify the problem, they are considered spherical. Two spherical bodies in contact with  $R_1$  and  $R_2$  radii have the effective radius defined as:

$$\frac{1}{\tilde{R}} = \frac{1}{R_1} + \frac{1}{R_2} \quad (1)$$

If elasticity modules of two particles are  $E_1$  and  $E_2$ , then the effective elasticity module will be defined by:

$$\frac{1}{E^*} = \frac{(1 - \nu_1^2)}{E_1} + \frac{(1 - \nu_2^2)}{E_2} \quad (2)$$

In which  $\nu$  is the poisson's ratio. Considering the Hertz contact model for two spheres in contact, the effective elasticity module for spherical geometry is as follows [5]:

$$E^* = \frac{F}{\delta_{Hertz}^{1.5} \tilde{R}} \quad (3)$$

Finally, the cell elasticity module can be calculated using Eq. (2); having AFM tip data and cell poisson's ratio.

### 2.2 Adhesion Force Between Cell and Tip

AFM tip-sample interaction is used to measure the surface adhesion force. Adhesion force magnitude between particles equals the force needed to separate them. Engaged forces between tip and sample surface lead to deflection or deviation of a cantilever and during sweeping, a detector determines the cantilever deflection. Through converting deflection to force unit, engaged forces between tip and surface are calculated. Reliable results of adhesion force obtained through AFM cantilever bending needs precise calibration of spring constant [18].

### 2.3 Viscoelastic Characteristics of Biological Cell

Obtaining viscoelastic properties can increase the precision of cell mechanics. Assuming that the resultant frequency from cantilever Lorentz force is near the first frequency response, the governing equation of tip motion  $q(t)$  when oscillates far from the particle surface is [6]:

$$\frac{\ddot{q}}{\omega_{far}^2} + \frac{1}{\omega_{far} Q_{far}} \dot{q} + q = \frac{F_{mag} \sin(\omega_{dr} t)}{k_{cant}} \quad (4)$$

where  $\omega_{far}$  is the cantilever resonance frequency (rad/s),  $Q_{far}$  is the quality factor far from the surface,  $\omega_{dr}$  is the cantilever driving frequency (rad/s),  $F_{mag}$  is the magnitude of the magnetic excitation force,  $k_{cant}$  is calibrated cantilever spring constant and  $\dot{q}$  is tip velocity.

Using Eq. (4) and data extracted from the experiments, viscoelastic parameters of the Kelvin-Vogit model can be obtained as [6]:

$$\begin{aligned}
k_{sample}^{dynamic} &= \left( \frac{k_{cant} A_{1far}}{Q_{far} A_1} \cos(\phi_1) - \frac{k_{cant} A_{1far}}{Q_{far} A_{1near}} \cos(\phi_{1near}) \right) \times \sqrt{1 - \frac{1}{4Q_{far}^2}} \\
c_{sample}^{dynamic} &= \left( \frac{k_{cant} A_{1far}}{Q_{far} A_1} \sin(\phi_1) - \frac{k_{cant} A_{1far}}{Q_{far} A_{1near}} \sin(\phi_{1near}) \right) \times \sqrt{1 - \frac{1}{4Q_{far}^2}}
\end{aligned} \tag{5}$$

where  $A_{1far}$  is oscillation amplitude,  $\phi_{1far}$  is the phase lag far from the sample surface and  $\omega_{near}$  is cantilever resonance frequency near the sample. Since forces and displacements are equivalents of stresses and strains, accordingly stress parameters of Kelvin-Voigt can be obtained from force ones. It is obvious that  $E_{sample}$  is the stress equivalent of  $k_{sample}^{dynamic}$  and the stress equivalent of  $c_{sample}^{dynamic}$  will be the viscosity coefficient  $\eta_{sample}$ .

As mentioned before, the indentation depth and the tip-sample interaction force are composed of two parts which are related to quasi-static and dynamic force. Based on those parts, stress and strain are defined as follows:

$$\mathcal{E}_{dynamic} = \frac{\delta_{dynamic}}{R_s - \delta_{dynamic}}, \quad \sigma_{dynamic} = \frac{F_{tip}^{dynamic}}{\pi a_{dynamic}^2} \tag{6}$$

where  $R_s$  is sample radius, and  $a_{dynamic}$  is contact surface radius. Indentation causes depth and contact radius which can be related by Eq. (7) according to Hertz viscoelastic theory developed in previous sections:

$$\delta = \frac{a^2}{\tilde{R}} \tag{7}$$

where  $\tilde{R}$  is effective radius defined previously. Since  $\delta = \delta_0 + \delta_{dynamic}$ , the contact radius can also be divided in two parts,  $a^2 = a_0^2 + a_{dynamic}^2$ . According to continuum mechanics for the Kelvin-Voigt model, the relations between stress and strain in model branches, spring and viscosity branches, and total applied stress and strain are:

$$\mathcal{E}_{dynamic} = \mathcal{E}_d = \mathcal{E}_s, \quad \sigma_{dynamic} = \sigma_d + \sigma_s \tag{8}$$

where  $\mathcal{E}_s$  and  $\mathcal{E}_d$  are related to spring and viscosity, respectively.  $\sigma_s$  and  $\sigma_d$  are also related stresses of spring and viscosity. Strain-stress relation for spring and viscosity branches are  $\sigma_s = E_{sample} \mathcal{E}_s$  and  $\sigma_d = \eta_{sample} \dot{\mathcal{E}}_d$ , respectively.

According to strain equality in two branches, it can obviously be concluded that contact radii due to each stress are also equal; so, if  $a_{dynamic}$ ,  $a_s$  and  $a_d$  are respectively the contact radii of dynamic indentation, spring and viscosity forces, this relation is established as follows:  $a_{dynamic} = a_s = a_d$ . Finally the relation for obtaining Kelvin-Voigt stress parameters is:

$$E_{sample} = \frac{k_{sample}^{dynamic}}{\pi \tilde{R}} \left( \frac{R_s - \delta_{dynamic}}{\delta_{dynamic}} \right), \quad \eta_{sample} = \frac{c_{sample}^{dynamic}}{\pi \tilde{R}} \left( \frac{R_s - \delta_{dynamic}}{\delta_{dynamic}} \right)^2 \tag{9}$$

### 3 Experiments Methods

In this part, the experiments, their results and the comprehensive analysis will be presented. In general, the process of conducting the test is shown in Fig. 1.

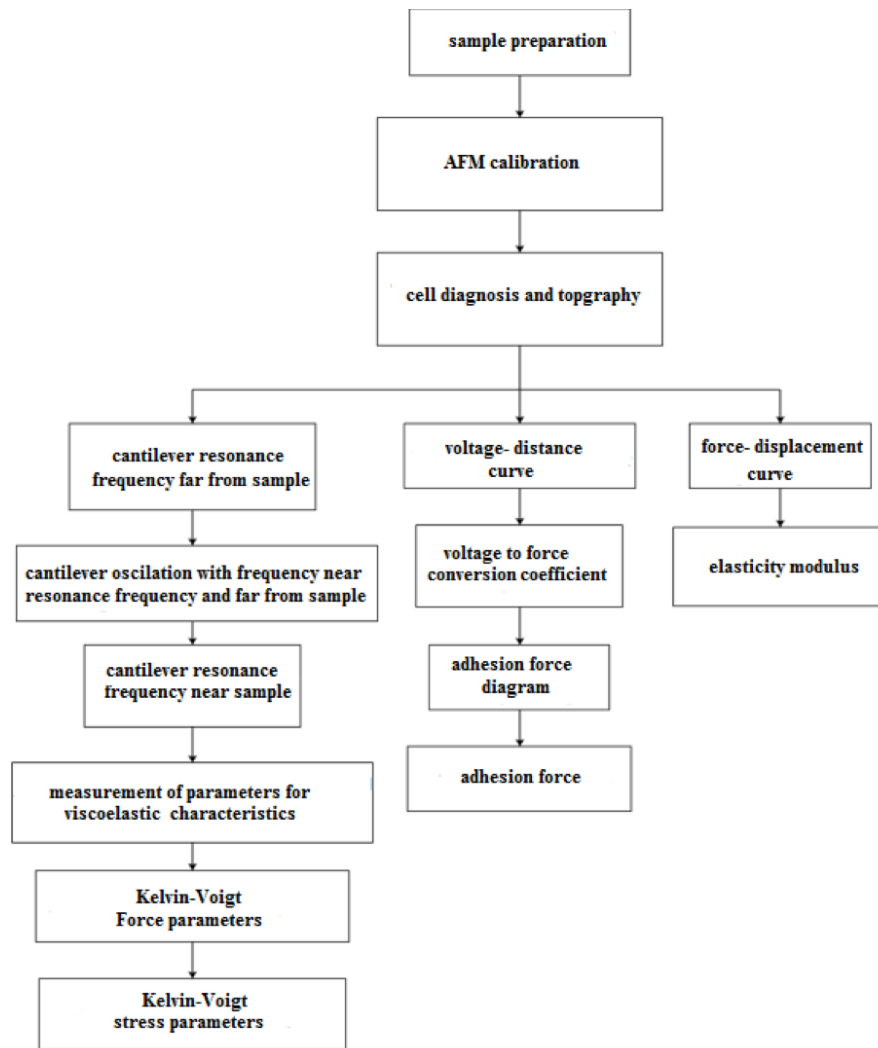


**Figure 1:** Experimental test flowchart

### 3.1 Sample Preparation

#### 3.1.1 MCF-10A Preparation

MCF-10A healthy breast cells were prepared in IBRC from a 36-year-old female. Cells were maintained in PHR-free DMEM/F12 culture medium, a week before the test. MCF-10A cells were provided in a volume of 70 ml and in order to separate them, 50 ml was kept in another test tube and the rest was poured away. The sample was washed out by PBS and 2 ml Trypsin was added. After keeping it 3 minutes in the incubator to complete the separation operation, 10 microliters of the sample dropped on the mica surface. Then, a special cap was put on the sample to prevent dusting.

#### 3.2 Devices and Initial Parameters

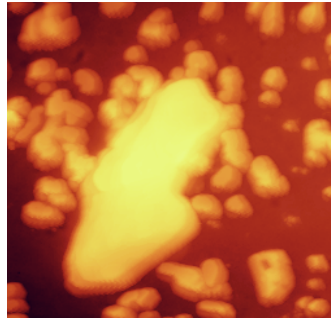
The tests were performed using ARA-AFM model No. 0101/A with the stimulation frequency of 278 Hz. We tried to indent the cells about 50 nm to avoid cell damage.

## 4 Results

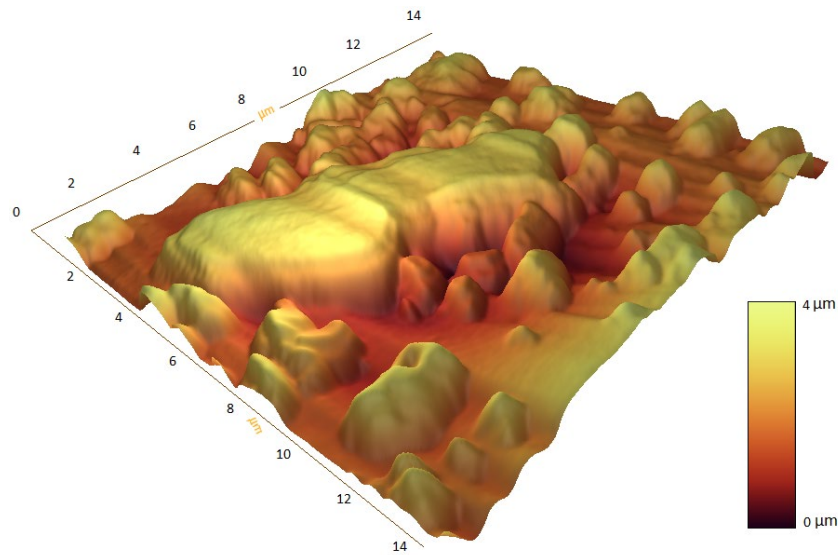
### 4.1 Cell Imaging and Topography

After locating the sample on its special position, a probe processes to identify surface properties. Then, processed images will be transferred to the computer connected to atomic force microscopy. Images are saved and recorded using the AFM software.

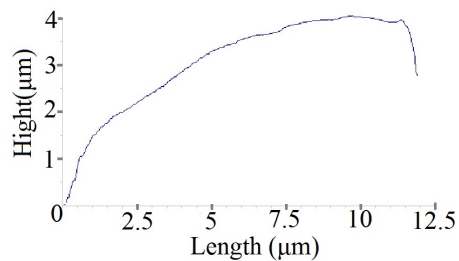
Geltmeier et al. reported the MCF-10A cells' volumes in  $678-1317 \mu\text{m}^3$  range [4]. Considering spherical geometry for these cells and careful attention to Fig. 2 specified that the tested cells are in this range so it can be said that we correctly identified MCF-10A cells.



(a) MCF-10A cell



(b) Cell 3D topography



(c) Cell surface profile

**Figure 2:** The overall view of the MCF-10A cell (a-c)

### 4.2 Elasticity Module

In this part, the experiment involves obtaining force-indentation curves for MCF-10A cells and the curves of three points with different thicknesses were obtained for six MCF-10A cells where three of less noisy cells were chosen. The elasticity modulus of each cell in three specified points were extracted using Hertz elastic theory while the cells were considered spherical.

The aim was to obtain changes rate of elasticity module in 3 points of a cell using existing theory and the assumption of the known poison's ratio.



**Figure 3:** The indented points of the MCF-10A cells

Cells are considered spherical with the poison's ratio of 0.4999 [4]. Having a spherical geometry, the atomic force microscopy probe has a poison's ratio of 0.27. The results based on Hertz contact theory are summarized in Tab. 1.

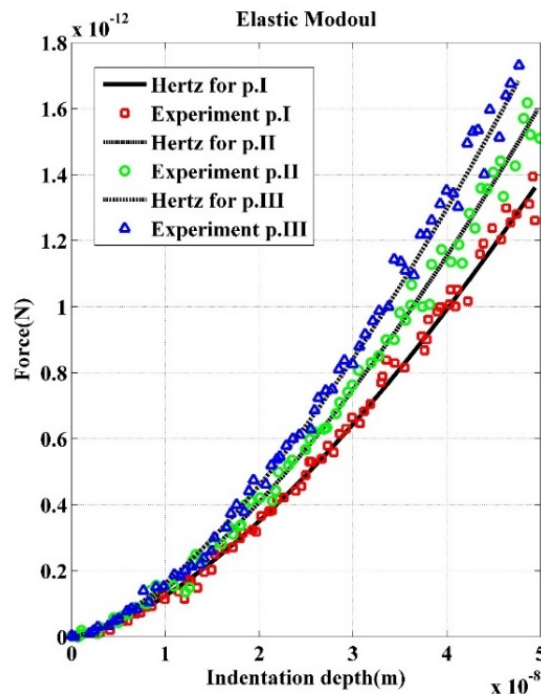


**Figure 4:** Experimental curves of the force-indentation depth for three points of the MCF-10A cells and estimation of elasticity module by Hertz theory

Experimental data and predicted force-indentation depth curves for the Hertz contact theory have been demonstrated in Fig. 4. According to Tab. 1 and Fig. 4, the cell elasticity module at the thinner edges is

higher and for the thicker points is lower. The outcome is similar to the result attained by Park and Lee [14], who used spherical probe AFM. As showed in Fig. 5, the AFM tip was put in contact with three different parts of the cell and force-indentation depth curves for every three parts were obtained accordingly. Considering AFM probe as a rigid sphere and the cell as an elastic body with the assumption of a known poisson's ratio, they utilized Hertz theory to calculate the elasticity module for every three parts. They concluded that the elasticity module of the thinner parts of the cell is higher. These results are reasonable since there is less intracellular liquid in the region with less thickness and so the membrane (which has similar behavior to solid materials) will be more effective and consequently, the elasticity module is higher compared to other regions (with higher thickness and more intracellular liquid). In addition, since point II has a higher thickness in comparison with the point I and point I is thicker than point III, subsequently, obtained module for point III is more than the two other points; also, the point I has a higher module in comparison with II.

Results for MCF-10A cells are the same as MCF-7 cells [9], i.e., cell elasticity module at parts with less thickness is higher and vice versa. It can be said repeatability and following a similar pattern for all three points of two cells confirm the results.

**Table 1:** Average elasticity modulus for three points of the MCF-10A cells (*kPa* )

MCF-10A Elasticity module	
Point I	1.31
Point II	1.51
Point III	1.83

### 4.3 Adhesion

By means of force spectroscopy, atomic force microscopy can measure interaction forces between the cantilever and its substrate. While moving up and down, the cantilever is bending because of forces between tip and sample and the force-distance curve will be obtained [2].

Piezo voltage-distance curves for different three points of both cells were obtained. Then, using the mentioned relations, adhesion force-distance curves were acquired for every three points of each cell. The goal was to obtain adhesion force changes rate in different points of a cell to make a comparison to specify the adhesion difference of the points. During the tests, humidity was about 28% and the tip was approaching the sample surface and getting away at the speed of 261.4 nm/s. Tab. 2 shows the summarized results.

**Table 2:** Average adhesion force of the cells in different points (*nN* )

Adhesion force of the MCF-10A	
Point I	139.41
Point II	172.41
Point III	54.89

The adhesion force-distance curves for cells in different points, during the approach of the tip to the sample, has been presented in Fig. 5.

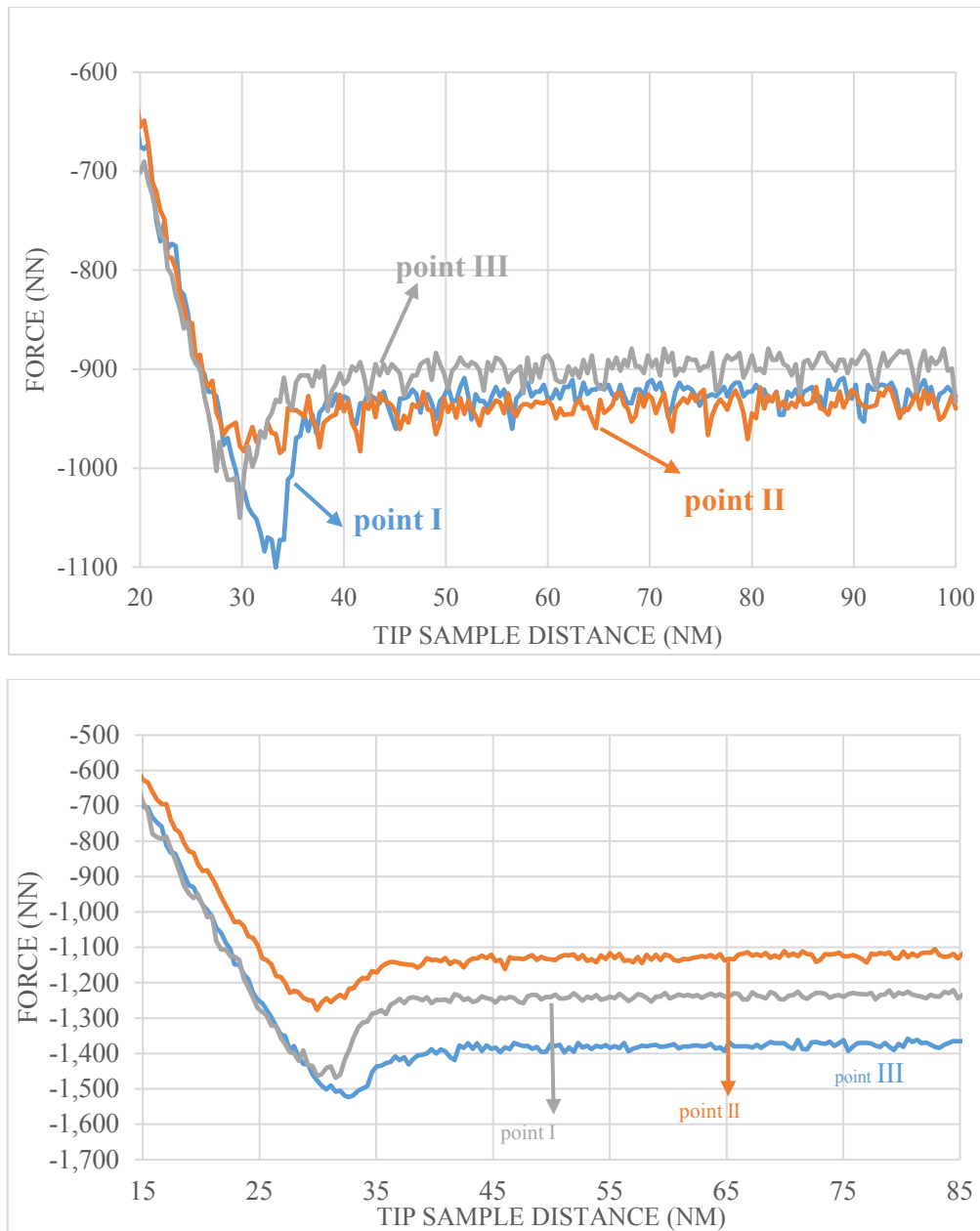


**Figure 5:** Adhesion force-distance curves for diverse points of two cells

According to Tab. 2 and Fig. 5, in general, for MCF-10A, the maximum magnitudes are for points I, II and III, respectively. These results show that softer parts are more adhesive compatible with MCF-7 results [9], so this repeatability confirms them.

**4.4 Viscoelastic Characteristics (Kelvin-Voigt Parameters)**

Following assumptions should be met during the test:

- I. The cantilever is moved directly with no oscillation or sample driving.
- II. The tip is in constant contact with the sample and oscillation amplitude is small in comparison with pure indentation of the tip in the sample.
- III. Special mode of cantilever oscillating far from the sample is constant in comparison with the time compressing the sample.

IV. It should be noted that hydrodynamic correction on a living cell is different compared to the fix one.

It can be observed that measured Kelvin-Voigt parameters highly depend on indentation depth; thus the increase in depth results in magnitude growth. Closer view implied that small drive frequency leads to higher Kelvin-Voigt parameters.

According to the repeatability of test results, it can be concluded that calculated results are correct and accurate. On the other hand, to confirm the results, they can be compared to Cartagena and Raman study who extracted local viscoelastic characteristics of fibroblast cells [1]. This comparison shows that the obtained trend in measurable harmonic parameters and next, Kelvin-Voigt parameters for both cells are similar to fibroblast cells results of Cartagena and Raman.

After obtaining Kelvin-Voigt force parameters using relation 5, their stress equivalents can be derived. Since the trend of the  $E_{sample}$  and  $\eta_{sample}$  are respectively similar to  $k_{sample}^{dynamic}$  and  $c_{sample}^{dynamic}$ , it is not necessary to address them here, instead, after calculation of Kelvin-Voigt stress parameters in different indentation depths for each cell, the time constant ( $\tau_{sample} = \eta_{sample} / E_{sample}$ ) for each cell will be calculated in different indentation depths.

Then, using  $C_{sample}(t) = (1/E_{sample})(1 - e^{-t/\tau_{sample}})$  (obtained from continuum mechanics and explained in previous sections) creep function magnitudes for different depths were calculated. Since working with different magnitudes of  $E_{sample}$  and  $\tau_{sample}$  for different depths is very difficult, an attempt was made to calculate a single  $E_{sample}$  and  $\tau_{sample}$  for each cell. These magnitudes should be selected in the way that the theoretical creep function matches the calculated creep function magnitudes for that cell. Since for this creep function, there are many magnitudes for  $E_{sample}$  and  $\tau_{sample}$ , it is simpler to designate a more familiar magnitude to one of these parameters.

The time constant for the first and second cells are 1.1 and 1.05 secs, respectively. Theoretical and experimental curves adaptation and repeatability of this magnitude confirm the results. Similar curves were obtained for MCF-10A which had analogous results to MCF-7 [9], showing the tests repeatability for different cells (Figs. 6 and 7).

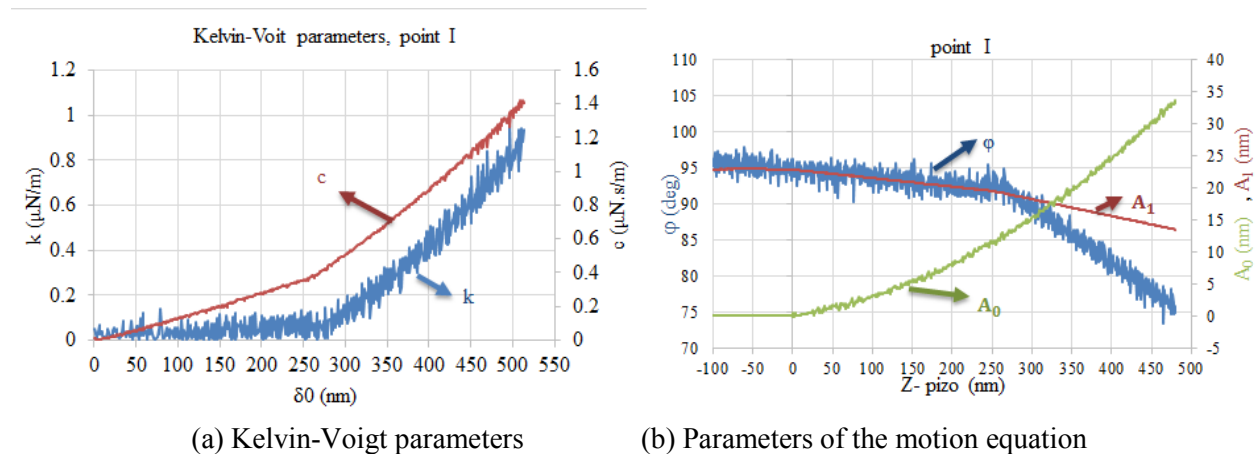
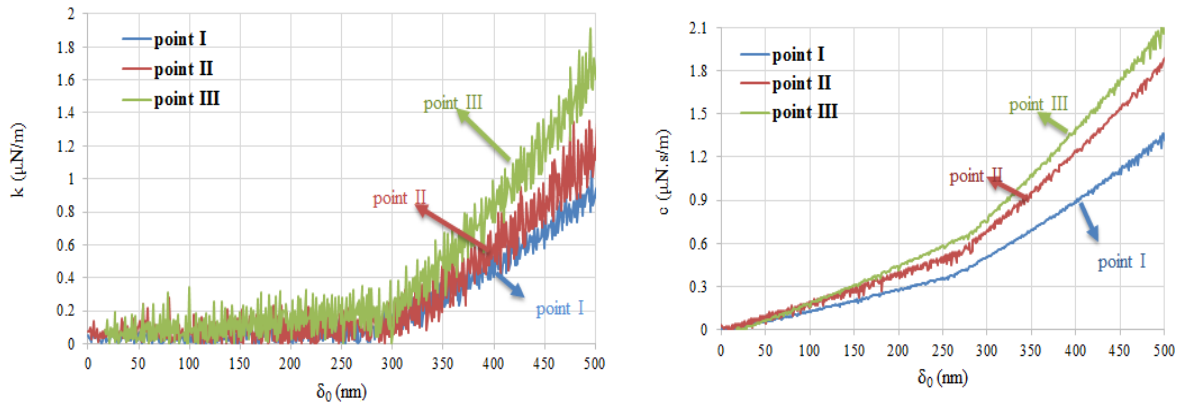


**Figure 6:** The curves of the approaching tip to the three different points and measurable parameters



(a) Spring constant of the three points (b) Viscosity coefficients of the three points

**Figure 7:** Kelvin-Voigt force parameters' comparison

In the previous section, the elasticity modulus for the central points of the MCF-10A cell was presented. As a result, with this assumption, the time constant for each point can be extracted. The theoretical and experimental creep function for three points have been presented (Fig. 8). The time constants were 1.42, 1.1 and 1.36 secs for the first, second and third points respectively. Acceptable compatibility of theoretical and experimental curves and repeatability of these magnitudes can confirm the obtained results.

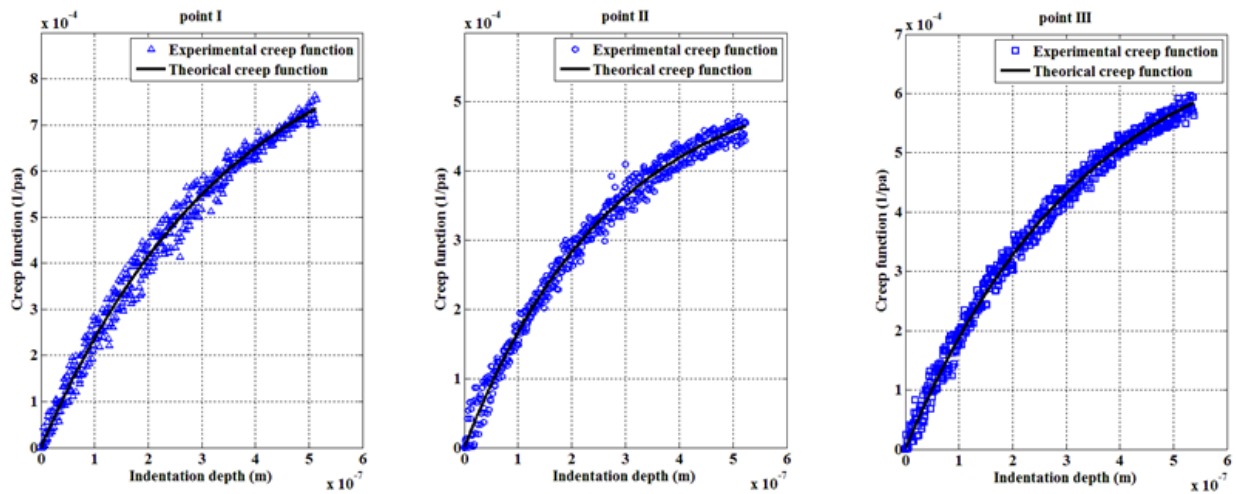


**Figure 8:** Theoretical and experimental creep functions for three points

#### 4.5 Axial Rigidity and Bending Rigidity

Axial and bending rigidities are properties that can be used in modeling of the cell manipulation by AFM. The accuracy leads to the precise modeling of the manipulation process and consequently, better prediction of the cell behavior. To obtain axial and bending rigidity, considering a spherical cell, a moment of inertia and area should be calculated first and then, using existing relations, the intended magnitudes will be extracted. According to the previous experimental results of the radius and elasticity module for breast cells and using existing relations for the moment of inertia, related bending and axial rigidities are achievable (Tab. 3).

#### 4.6 Comparison Between the Cancerous and Healthy Breast Cells' Results

Comparison between healthy and cancerous cells can assist in disease's diagnosis, prevention, and therapy; owing to the fact that immediately after characterization of the sampled cell and through observing the changes, the treatment can be initiated.

To compare the elastic properties' differences between cancer cells and their counterpart normal cells, the relative Young's modulus ( $E_R$ ) is defined as follows:

$$E_R = E_{\text{cancer cell}} / E_{\text{counterpart normal cell}} \quad (10)$$

where  $E_{\text{cancer cell}}$  and  $E_{\text{counterpart normal cell}}$  are Young's moduli of the cancerous and normal cells, respectively. The results of this paper show that the relative Young's modulus is about 0.75 which shows the softness of cancer cell in comparison with a normal one. Higher relative modulus indicates less cancer progress and this magnitude helps diagnosis of cancer level.

**Table 3:** Comparison between the MCF-7 and MCF-10A properties

	<i>Radius</i>	<i>Elasticity module</i>	<i>Adhesion force</i>	<i>Bending rigidity</i>	<i>Axial rigidity</i>
<i>MCF-10A</i>	$\sim 6.25\mu\text{m}$	$1.60\text{kPa}$	$150.47\text{nN}$	$64.47 \times 10^{-27}$	$0.589 \times 10^{-12}$
<i>MCF-7</i>	$\sim 7.16\mu\text{m}$	$1.203\text{kPa}$	$165.43\text{nN}$	$203.2 \times 10^{-27}$	$0.87 \times 10^{-12}$

Based on Tab. 3, the healthy breast cells (MCF-10A) in comparison with the cancerous ones (MCF-7) are stiffer and less adhesive. As may be inferred from the images of the optical and atomic force microscopy, healthy cells are smaller but more stretched (Fig. 9).

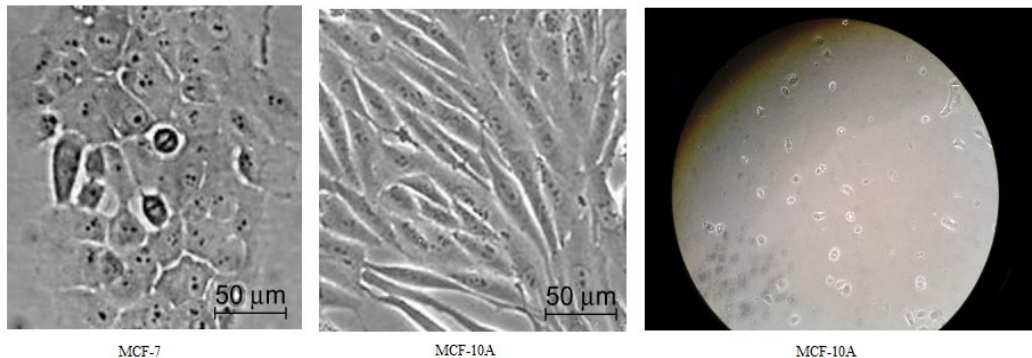


**Figure 9:** Healthy and cancerous cells

## 5 Discussion

Investigation of biological cells' apparent properties, especially cancer cells, can increase accuracy in treatment and prediction of their behavior, consequently helping the diagnosis of different types of cancer. Breast cancer is one of the most common cancers among woman. Atomic force microscopy is among the most powerful tools in imaging and characterization of Nano-particles. Mechanical properties of many biological cells have been extracted using various methods but comprehensive experiments for healthy and cancerous breast cells have not been done simultaneously. In this paper topography and mechanical properties of MCF-10A cells such as elasticity modulus, adhesion force and viscoelastic characteristics have been extracted and used to investigate axial and bending rigidity through AFM. Initially, topography and the apparent properties of these cells have been investigated and the obtained results were then compared with the previous studies for confirmation.

After accurate recognition of MCF-10A cells, the elasticity module was evaluated. To simplify the calculation process, cells were considered as spheres. In this step, the aim was finding the rate of elasticity module changes in various points of the cell. Force-indentation depth curves for three different points on cells were obtained. Afterwards, using Hertz elastic theory, the elasticity module of each cell at three points was extracted. Results showed that the elasticity module at the thinner parts were higher and the points with higher thickness had lower modules. Lastly, the points with average thickness (points D) have elasticity module between these two magnitudes. It was also demonstrated that thicker parts which contained more liquid were softer and the edges of cells with less liquid had higher elasticity modules.

Adhesion force is one of the crucial factors in friction force development; consequently, the next test was to obtain the adhesion between cell and tip. Generally, the maximum magnitudes of adhesion were recognized at softer points and vice versa. The usual method for extracting cell elastic properties is AFM force-indentation depth curves. Obtaining viscoelastic characteristics can increase the accuracy of cell mechanics. Viscoelastic characteristics are obtained from dynamic methods. In this paper, spring force and viscosity gradient, and as a result stiffness and viscosity mechanical properties were measured in different indentation depths. Kelvin-Voigt was used as the cell mechanics model. After obtaining force parameters of Kelvin-Voigt, stiffness and viscosity, their equivalents in stress-strain relations were found. Through calculating the stress parameters of Kelvin-Voigt at different indentation depths for each cell, a time constant of each cell were calculated. Then, creep function magnitudes for different depths were calculated and attempt was made to extract a suitable and unique creep function for each cell which is in line with the theoretical creep function. The suitable creep functions for MCF-10A cells were discovered, representing their viscoelastic behavior.

Finally, axial and bending rigidities were obtained and compared for two cells considering the spherical geometry and the elasticity module. According to elasticity modulus and adhesion, the points with lowest adhesion and highest elasticity modulus were chosen as the optimum points for starting manipulation, because lower adhesion needs a smaller force for separation from the surface. On the other hand, higher elasticity modulus (stiffer part) results in smaller deformation under the same applied force; therefore, the possibility of damage or destruction will decrease. Moreover, the comparison between MCF-7 and MCF-10A cells revealed that MCF-7 cells were softer and less adhesive. These results can be used for the diagnosis of cancerous cells and also their progress. In addition, manipulation of biological cells is a process requires accurate modeling and simulation to predict cells' and tools' behavior during experiments; hence, these properties can help in order to achieve a precise modeling and prediction.

**Conflict of interest:** The authors declare that they have no conflict of interest.

## References

1. Cartagena A. Local viscoelastic properties of live cells investigated using dynamic and quasi static atomic force microscopy methods. *Biophysical* **2014**,106: 1033-1043.
2. Çolak A. Measuring adhesion forces between hydrophilic surfaces with atomic force microscopy using flat tips. 1st ed. Physics of Interfaces and Nano-Materials Group, University of Twente. **2013**.
3. Faria EC, Ma N, Gazi E, Gardner P, Brown M et al. Measurement of elastic properties of prostate cancer cells using AFM. *Analyst* **2008**,133: 1498-1500.
4. Geltmeier A, Rinner B, Bade D, Meditz K, Witt R et al. Characterization of dynamic behavior of MCF7 and MCF10A cells in ultrasonic field using modal and harmonic analyses. *PLoS One* **2015**, 4: 1-20.
5. Hertz H. Über die Berührung fester elastischer Körper. *Journal für die reine und angewandte Mathematik* **1881**, 92: 156-171.
6. Hui CY, Baney JM. Contact mechanics and adhesion of viscoelastic spheres. *Langmuir* **1998**, 14: 6570-6578.
7. Ikai A, Afrin R, Sekiguchi H, Okajima T, Alam MT. Nano-mechanical methods in biochemistry using atomic force microscopy. *Current Nanoscience* **2003**, 4: 181-193.

8. Kasas S, Longo G, Dietler G. Mechanical properties of biological specimens explored by atomic force microscopy. *Journal of Physics, D: Applied Physics* **2013**, 46: 1-12.
9. Korayem MH, Sooha YH, Rastegar Z. MCF-7 cancer cell apparent properties and viscoelastic characteristics measurement using AFM. *Journal of the Brazilian Society of Mechanical Sciences and Engineering* **2018**, 40: 297.
10. Korayem MH, Khaksar H, Taheri M. Modeling of contact theories for the manipulation of biological micro/nanoparticles in the form of circular crowned rollers based on the atomic force microscope. *Journal of Applied Physics* **2013**, 114: 1-10.
11. Li M, Liu L, Xi N, Wang Y, Dong Z et al. Atomic force microscopy imaging and mechanical properties measurement of red blood cells and aggressive cancer cells. *Science China Life Sciences* **2012**, 55: 968-973.
12. Li QS, Lee GYH, Ong CN, Lim CT. AFM indentation study of breast cancer cells. *Biochemical and Biophysical Research Communications* **2008**, 374: 609-613.
13. Louey MD, Mulvaney P, Tewart PJS. Characterization of adhesive properties of lactose carriers using atomic force microscopy. *Journal of Pharmaceutical and Biomedical Analysis* **2001**, 25: 559-567.
14. Park S, Lee YJ. Nano-mechanical compliance of müller cells investigated by atomic force microscopy. *International Journal of Biological Science* **2013**, 9: 546-554.
15. Puech H, Taubenberger A, Ulrich F, Krieg M, Muller DJ et al. Measuring cell adhesion forces of primary gastrulating cells from zebra-fish using atomic force microscopy. *Journal of Cell Science* **2005**, 118: 4199-4206.
16. Rodriguez ML, McGarry PJ, Sniadecki NJ. Review on cell mechanics: experimental and modeling approaches. *Applied Mechanics Reviews* **2013**, 65: 060801.
17. Siamantouras E, Hills E, Squires PE, Liu K. Nano-mechanical investigation of soft biological cell adhesion using atomic force microscopy. *Cellular and Molecular Bioengineering* **2014**, 8: 22-31.
18. Stegemann B, Backhaus H, Kloss H, Santner E. Spherical AFM probes for adhesion force measurements on metal single crystals. *Modern Research and Educational Topics in Microscopy* **2007**, 64: 820-827.
19. Vinckier A, Semenza G. Measuring elasticity of biological materials by atomic force microscopy. *FEBS Letters* **1998**, 430: 12-16.
20. Weisenhorn AL, Khorsandi M, Kasas S, Gotzos V, Butt HJ. Deformation and height anomaly of soft surfaces studied with an AFM. *Nanotechnology* **1993**, 4: 106-113.
21. Zhai M, McKenna GB. Viscoelastic modeling of Nano-indentation experiments: a multi-curve method. *Journal of Polymer Science Part* **2014**, 52: 633-639.